INVESTIGATING TERRESTRIAL LASER SCANNING INTENSITY DATA: QUALITY AND FUNCTIONAL RELATIONS

Norbert Pfeifer[a], Peter Dorninger[a], Alexander Haring[b], Hongchao Fan[b]
[a]Institute of Photogrammetry and Remote Sensing
[b]Christian Doppler Laboratory "Spatial Data from Laser Scanning and Remote Sensing"
Vienna University of Technology, 1040 Vienna, Austria
{np, pdo, ah, hf}@ipf.tuwien.ac.at

KEY WORDS: Terrestrial Laser Scanning, Intensity, Radiometry, Quality.

ABSTRACT
Terrestrial laser scanning is primarily used for recording dense cloud of points on objects. However, laser scanners record the optical power of the backscattered echo of the emitted signal, too. These values are supplied as so-called intensity. The intensity values are investigated systematically for one scanner (Riegl LMS-Z420i). For doing so, we use targets with known reflectivity and scattering characteristics. It shows that an inverse-square-law, relating intensity to range, is too simple. An empirical data driven model is thus derived and results are compared to the physical model. For our experiment, covering a distance range of 1.2-48m, angle of incidence 0-70°, and target reflectivity 5-99%, the intensity values in the range [0.1,0.3] could be predicted with a r.m.s.e. of 0.011.

1 INTRODUCTION

Terrestrial laser scanning (TLS) has found wide-spread use for acquiring geometric information for applications in cultural heritage documentation, open pit mining, or reverse engineering. Applications encountered less often include, e.g., forestry, forensics, deformation measurements, or glacier monitoring. The LiDAR (light detection and ranging) principle allows, however, to extract more information on a target than only a range image. The term target refers to the object that scatters back the emitted beam. The information beyond range is primarily the reflectance of the object, where reflectance is the ratio of backscattered to incident radiation at the wavelength of the laser (Jelalian, 1992) at the angle of incidence. More specifically, the target cross section can be determined free of assumptions whereas reflectance can be determined based on assumption about scattering characteristics. Target movement and vibration additionally cause a frequency shift and spectral broadening in the backscatter. These principles are used for airborne and terrestrial meteorological studies (Weitkamp, 2006). This paper concentrates on the so-called intensity values acquired by terrestrial laser scanners. The intensity is a measure of the electronic signal strength obtained by converting and amplifying the backscattered optical power. These measurements are rarely used, and most commonly their purpose is to support the visual analysis of a point cloud. However, they have a potential for more sophisticated applications such as registration or classification by surface material property.
In this contribution we primarily want to systematically investigate the quality of these intensity values. Additionally, we want to investigate a possible influence on distance measurement. The possibility to reconstruct non-geometrical surface properties will be touched as well. For performing these investigations we suggest a dedicated experimental setup and demonstrate it.
In airborne laser scanning first steps are made for the exploitation of the intensity, exemplified e.g. by the contributions of Wagner et al. (2006) and Jutzi et al. (2006). For terrestrial scanners this is – in principle – possible too, and should be exploited where appropriate. Some problems are currently hindering the direct exploitation. It is, e.g., not necessarily the case that the received power is mapped linear to an intensity value, e.g. due to saturation effects, and the variations in emitted

power are not known either. Therefore, the investigation of the "radiometric behavior" of terrestrial laser scanners is a first step for a further exploitation of these observations. The quality allows deciding if certain applications, e.g. classification based on intensity or surface reflectance, can be performed or not. One such scenario, which will not be treated in this contribution, could be the determination of surface properties (e.g. water content in sand).
Furthermore, as it has been reported by many authors (e.g., Valanis et al, 2004, Hanke et al., 2006) the backscatter strength has a systematic influence on the range measurement, therefore, the acquired geometry is affected by the radiometry. These studies pointed out effects, but the experiments performed were not aimed at isolating them. This is the aim of our contribution. The work presented also complements the work performed e.g. by the group at FGAN FOM, investigating terrestrial laser scanning from a more physical point of view.
Firstly we concentrate on the radiometric measurement quality, i.e., not considering range as the variable of interest, but the "intensity value". Investigations of that effect have been conducted before, but often the result are discussed with reference to 'color' whereas the monochromatic nature of the laser light, often not in the visible range, is neglected. Also the surface structure on the microscopic level influences these measurements (Jutzi and Stilla, 2003), which makes it therefore difficult to separate the effects. For materials like marble the penetration of the laser into the object has been described by Godin et al. (2001), for other materials, e.g. styrofoam it is quite obvious. We describe an experiment making use of a material that is

- reflecting on the top surface, i.e. there is no penetration into the material,
- has a well defined, i.e., known, reflectance at the laser wavelength, and
- shows purely diffuse reflection, i.e., is a Lambertian reflector.

Additionally, the background radiation is controlled, i.e. excluded in some of the experiments. The radiometric quality is analyzed almost over the entire range of diffuse reflection, in the range of 5% to 99% of reflectance, and for one retroreflective material.
Additionally, the impact of radiometric quality on geometric measurement quality is investigated. We will report effects which have been observed by other authors also in the past. However, our experiments are specifically designed to observe and study these effects.
For the above aims well-defined, repeatable experiments are performed with one terrestrial laser scanner, employing the principles of pulse round trip time laser range finding. Looking at intensity images of phase-based laser scanning, the noise appears to be smaller compared to intensity images acquired from pulse round trip time scanning. We did not perform experiments to quantify (and validate) this assumption, however.
In the next section the physical background will be laid out. Then the experiment is described and the results will be discussed.

2 PHYSICAL BACKGROUND

Pulsed laser scanners analyze the echo of an emitted pulse. In the static case, i.e., temporal variations of the pulse power are neglected, the emitted power P_E and the received power P_R are related by the laser equation (Jelalian, 1992). If the surface scattering back the radiation is larger than the beam footprint, the target is a so-called extended target. If, furthermore, the target is a Lambertian reflector, the backscatter strength in the angular domain depends only on the angle of incidence α (i.e., angle between surface normal and laser ray traveling from the target to the detector). The laser range equation then becomes.

$$P_R = \pi P_E \rho \cos(\alpha) / (4r^2) \ \eta_{Atm}\eta_{Sys} .$$

The term ρ is the reflectance of the material, i.e. a surface material property, and the η-terms describe the atmospheric and system transmission factor. An extended target that would scatter all the incident radiation to the detector would reduce the equation to $P_R = P_E \ \eta_{Atm}\eta_{Sys}$. However, retroreflective targets, especially those made of foil, usually also have some portion of scattering in other directions than the incident ray direction.

There is a number of assumptions in the laser range equation as written above. Firstly, only extended targets are used. The beam width, therefore, does not appear in the laser range equation. For non extended target also the deviation from a linearly expanding footprint in the near field of the aperture would have to be considered (Jelalian, 1992). Additionally, it is assumed that the receiver has exactly the same field of view as the emitter, which can be true for mono-static systems. It is practically true for quasi mono-static systems, where the receiver and the emitter are in close proximity, for long ranges (Bae and Lichti, 2005). For shorter ranges the consequence is that the emitter and receiver instantaneous field of view are not coincident.
At the ranges used in the experiments (max. 50m one way) the atmospheric transmission factor, using a standard clear atmosphere, does not fall below 99% and was therefore neglected. Under the assumption of a constant, but unknown power emitted for each pulse the laser range equation under the conditions for Lambertian targets can be rewritten as
$i = \rho \cos(\alpha) / r^2 \, \eta_{Sys} \, C$.
where i is the intensity and C is an unknown factor. The term η_{Sys} is not necessarily a constant. Next to a linear amplification, logarithmic or other system transmission functions may be found.

3 EXPERIMENT SETUP

Lambertian targets with a size of 12.7x12.7cm^2 at reflectance of 5%, 20%, 40%, 60%, 80%, and 99% were available. The target base material is Spectralon, featuring the properties listed in the introduction, obtained from Laser2000 (www.laser2000.de). Additionally retroreflective foil in circular shape with 4cm diameter was used. No special information on the degree of reflection or the scattering characteristics was available. Two structures for mounting the targets were used.
The first structure is a metal frame that can be fixed to a tripod used for standard geodetic equipment. The frame was constructed such that the target surfaces lie in one plane. This planarity was not quantified, but visual inspection indicated, that this was reached with a precision better than ±1mm. Rotation of the frame with an accuracy of about ±2° (estimated) could be realized with the help of marks in 5° steps. The vertical bars of the metal frame were not masked by the Lambertian targets and small plastic bars were attached to these bars to establish a plane that included the target surfaces and the plastic bars. This plane was established with an accuracy of about ±1mm (estimated). The plastic bars were carrying markers that could be identified in the laser scanning intensity data. They were used to establish a coordinate system. The xy-plane of this coordinate system was parallel to the target plane and a possible (constant) offset is in the order of 1mm. This is shown in Fig. 1.

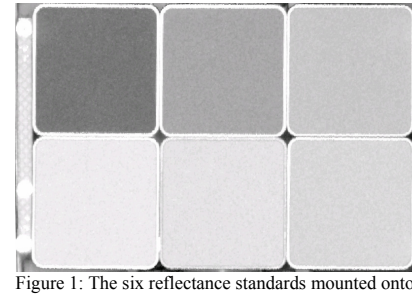

Figure 1: The six reflectance standards mounted onto a frame with four reference points in the corners (bright white).

The second construction was a plastic plate with square holes for the targets. The distance between the edges of adjacent holes was about 5cm. On top of the plate the retroreflective target was placed for one of the experiments. The thickness of that target was well below 1mm.
Scanning was always performed with the highest possible density, i.e. an angular resolution of 0.004°. Scanning was performed in a laboratory, which did not have temperature or humidity control. A window was set manually in the scanner control software to scan only the frame.
After manually picking points on the markers in the laser scanner intensity images the coordinate systems of the measurement frames could be reconstructed. Then the target areas were selected automatically, considering the footprint diameter at the maximum distance to avoid including measurements over more than one surface material. This resulted in 350 to 3900 points per target,

depending on distance and incidence angle. For the retroreflective target the points were selected manually by drawing a fence. The automatically selected points were used to fit planes minimizing the orthogonal distances. With this plane the incidence angle for each measurement ray was calculated. The points were exported in a Cartesian coordinate system with the origin in the scanner and the intensity as real number in the range [0,1]. These ASCII files were analyzed in Matlab.
The following experiments were performed.

Ex1: The plastic plate with the six Lambertian targets was measured in distances of 2.5m, 3m and in 1m-steps up to 16m. The frame was oriented to directly face the scanner and rotated by 45° against it.

Ex2: The metal frame was placed in a distance of 5m from the scanner and rotated in steps of 4.5° from 0° up to 54°.

Ex3: The plastic plate with the six Lambertian targets was placed in distances of 1.2m, 1.8m, 2.5m, 12m, 15m, 16m, 21.8m, 26.8m, 28.2m, 35.8m, and 46.8m, directly facing the scanner. The values were chosen to find the shortest and longest range allowing measurement to all targets. The length of the laboratory was the determining limit for the longest ranges.

Ex4: The metal frame was placed in a distance of 5m from the scanner and rotated to 0°, 40°, 54°, 63°, and 72°.

Ex5: Experiment like **Ex4** but all light sources (bulbs and fluorescent tubes) turned off.

Ex6: The retroreflective target was observed on the plastic plate at the distances used in **Ex3**.

The first two experiments were performed on one day, the others 10 days later. The experiments **Ex3** and **Ex6** were performed simultaneously. Likewise, experiments **Ex4** and **Ex5** were performed simultaneously, by alternately turning on/off all light sources. One such experiment is therefore one set of observations to be analyzed, containing multiple scans.
From the reported measurements (range and intensity) to each target, at the different ranges, incidence angles, etc., the following figures were extracted.
I : mean of the intensity values
s_I : standard deviation of the intensity values
r : mean of the range values
e : mean of the signed distances from the points on the target to the common plane of one frame
α : mean of the incidence angles
Additionally, for each target the reflectivity ρ is known. The laser scanner used for the experiments was a Riegl LMS 420i (Riegl, 2007).

4 ANALYSIS

The data acquired was used to study the relation between range, reflectivity, intensity, standard deviation of intensity, and systematic error in range measurement, using the computed angle of incidence, the known target reflectivity, and the measured range as parameters.

4.1 Intensity Standard Deviation

The standard deviation of the intensity values s_I observed in the experiments depend primarily on the intensity value I themselves, see Fig. 2. Intensity values of experiments **Ex1-5** are in the range [0.112,0.312], which is only 20% of the nominally available range. Larger intensity values could not be observed with the diffuse reflecting targets, however. The standard deviations of these intensity values per target are in the range [0.0026,0.0086]. Mean values are given in Table 1.

As Fig. 2 shows, intensity values have the smallest standard deviation at I=0.14 with s_I=0.0026. For lower and higher values of intensity the standard deviations rise. The figure suggests that the spread of the standard deviation rises for higher intensity values, too. For the values observed, the standard deviation is always lower than 3% of the absolute value.

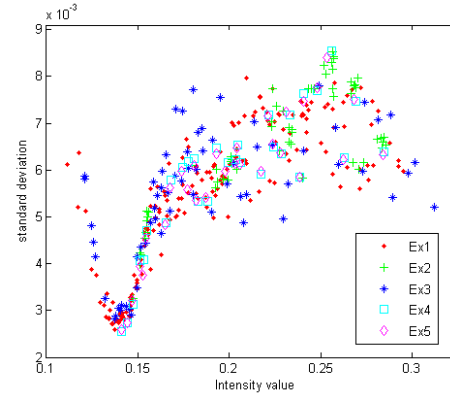

Figure 2: Standard dev. of intensity values s_I vs. intensity I.

In **Ex6** with the retroreflecting foil targets, the intensity values are in the range [0.541,0.725]. The standard deviation is in the range of [0.021,0.089]. This is ten times higher than the standard deviation found at the Lambertian targets, but intensity is higher by a factor of about three, too. On average I decreased with increase in r.

These results suggest that lower intensity values can be measured more accurately. We conclude that if a property related to backscatter strength of an extended target shall be observed with that laser scanner, then the distance (or angle of incidence) should be chosen in a way to reach the indicated optimal intensity value. This will provide the smallest uncertainty in intensity values.

For airborne laser scanning data Höfle and Pfeifer (2007) estimated for an Optech ALTM 2033, that the standard deviation of intensity values is 10% of the intensity itself. However, in that case no targets but natural homogeneous areas were used, featuring some heterogeneity in themselves.

4.2 Laser Range Equation and Intensity Values

The laser range equation, simplified as above, was used to test the assumptions associated with its application by establishing a relation between the backscatter strength and the intensity. For each target in each scan the value $p_R = \rho \cos(\alpha) / r^2$ was computed, which is – under the assumptions – linear proportional to the power reaching the detector. In Fig. 3 intensity is shown against p_R.

Ex4 and **5** show practically the same values, which was to be expected, as only the influence of background radiation may have influenced the difference. Also the measurements of the other "angle"-experiment, **Ex2**, fit to these values, and so do the observations of **Ex1** for the medium ranges [4m,14m]. The very short and very long ranges do not fit that well to an overall functional relation based on the laser range equation, which would appear as one curve in Fig. 3.

Different models relating p_R to I were tested, for each experiment individually and for different combinations of experiments. Logarithmic models always proved superior, compared to linear and higher order polynomial models. A logarithmic model appears as straight line in Fig. 3. Linear least squares adjustment using the observation equations of the form

$$I + v = \ln(p_R)\, x_1 + x_2$$

with x_1, x_2 the unknowns, and v the residuals (as vector: $\mathbf{v}$) were performed. No special weighting was applied for minimizing the square sum of residuals. The quality of the fit was evaluated with $\sigma_0 = (\mathbf{v}^T\mathbf{v}/(n\text{-}2))^{0.5}$, with n the number of equations.

Table 1 gives the results of adjustment as well as figures indicating the distribution of the intensity values. For **Ex2** the fit is best, with σ_0 similar to the standard deviation of intensity values. While this is an indication of the validity of the model, it has to be mentioned, that the intensity values show the smallest interval width.

Generally, σ_0 grows with the range of intensity values observed. Also, the multiplicative factor x_1 varies strongly between different groups of experiments. The observations from the graphic display in Fig. 3 are verified

The Experiments **Ex1,2,4,5** fit together. The quality of the fit, σ_0, is 0.0165, which is about three times the standard deviation of the intensity values s_I. This model may only be applied to data acquired with that specific scanner in the limited range of 2.5m to 16m and for intensity values between 0.1 and 0.3. Reducing the set to **Ex2,4,5** (limiting range and intensity spread) improves σ_0 by 15%.

Höfle et al. (2007) report an experiment similar to **Ex4** with an Optech ILRIS3D laser scanner, where one target with near Lambertian scattering characteristics in approx. 7m distance was observed at different angles. For incidence angles up to 70° the variation in intensity could be explained using the cosine-correction and a linear amplification model. Intensity values after the correction fitted together with half the spread found in the average intensity values of a single target measurement. Reshetyuk (2006), using an Leica HDS 3000, observed intensity decreased based on increased angle of incidence, but the target (a wall) was apparently not Lambertian. Bucksch et al. (2007) derived for a Faro scanner scattering characteristics of test charts, relating the intensity to the incidence angle. In the latter two experiments, intensity values were used directly, i.e. no special consideration was given to the unknown amplification of the received optical power.

However, **Ex3**, covering the largest range of distances between scanner and targets, but also featuring the highest intensity value, fits poorly to the other experiments. In Fig. 3 this corresponds to the long and short ranges on the left and right hand side of the figure, respectively. It has to be noted, that the range of 2m is below the measurement capability according to the system specifications. It is obvious that omitting those distances only does not improve the fit considerably.

The logarithmic model describing **Ex1-5** best has σ_0=0.0227. This is about four times the spread found in the intensity values for a homogeneous target. As systematic deviations are present, alternative, data driven models were investigated.

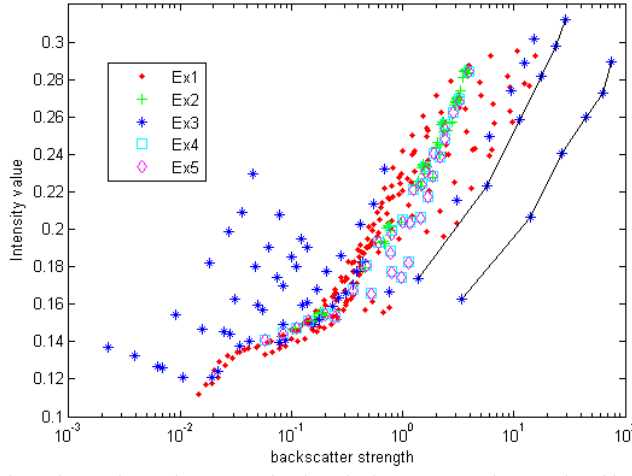

Figure 3: Intensity value against values proportional to backscatter strength on a logarithmic axis. The 2x6 measurements from **Ex3** on the right connected by a line are measurements to targets at ranges below two meter.

Data	Min(I)	Max(I)	Average s_I	n	x_1	x_2	σ_0
Ex1	0.1116	0.2954	0.0055	180	0.0284	0.2126	0.0165
Ex2	0.1472	0.2858	0.0066	66	0.0407	0.2190	0.0078
Ex3	0.1210	0.3121	0.0055	60	0.0160	0.2098	0.0271
Ex4	0.1411	0.2846	0.0059	30	0.0332	0.2093	0.0163

Ex5	0.1410	0.2840	0.0058	30	0.0330	0.2087	0.0163
Ex2,4,5	0.1410	0.2858	0.0062	120	0.0375	0.2148	0.0140
Ex1,2,4,5	0.1116	0.2954	0.0058	300	0.0307	0.2145	0.0165
Ex1-5	0.1116	0.3121	0.0057	366	0.0239	0.2131	0.0227
Ex1-5, r>2m	0.1116	0.3018	0.0057	354	0.0252	0.2151	0.0216

Table 1: Parameters and quality figures of logarithmic models relating the backscatter strength p_R to the intensity value.

4.3 Empirical Model for Intensity Values

While the physically induced model holds under certain circumstances, it indicates that the assumptions listed in Sec. 2 do not hold in general. Especially a range dependence other than the inverse square law is indicated.

Therefore, data driven models were investigated. A function F(ρ, α, r) is sought that predicts the intensity value from range, reflectivity, and incidence angle. The reasoning for limiting the number of possible models F was:

1. The influence of incidence angle and target reflectivity were *not* separated. Therefore the term ρ cos(α) was not split into two variables. For Lambertian reflectors and small footprints, the angle is considered similar to a change in reflectivity.
2. The influence of reflectivity and incidence angle on the one hand, should, however, be separable from the influence of range on the other hand.
3. Models should be as simple as possible, using low order polynomials, logarithmic and exponential functions. The number of parameters should be small to avoid over-fitting.

The final models can also be judged on the basis of the r.m.s.e., where the residuals v (**v** as vector) are defined as before

$$I + v = \mathrm{F}(\rho, \alpha, r).$$

This leads to $\sigma_0 = (\mathbf{v}^T\mathbf{v}/(n-u))^{0.5}$, with u the number of parameters of F.

In Fig. 4, left, the intensity values are plotted against range for **Ex3** only. The curves for the targets of different reflectivity show the same features. For short ranges below 2m the recorded intensity grows, drops until 20m, and increases for longer ranges again. A similar behavior, featuring an increase in intensity for ranges up to 4m and a linear drop thereafter, was observed also for a Faro phase-based scanner (Bucksch, 2007).

Different functions, including 1/ρ, more precisely 1/(ρ cos(α)), were tested. The function bringing the curves to the closest overlap was $(\rho \cos(\alpha))^{-0.16}$. In Fig. 4, right, the observations of **Ex1-5** are shown. All intensity values were multiplied with $(\rho \cos(\alpha))^{-0.16}$ to remove the influence of target reflectivity and angle of incidence. Then, the measurements were grouped in intervals of 2m width. For each class the mean, the standard deviation, and the coefficient of variation are plotted. For comparison the best logarithmic model (0.22/ln(ρ cos(α)) + 0.15) is shown, too.

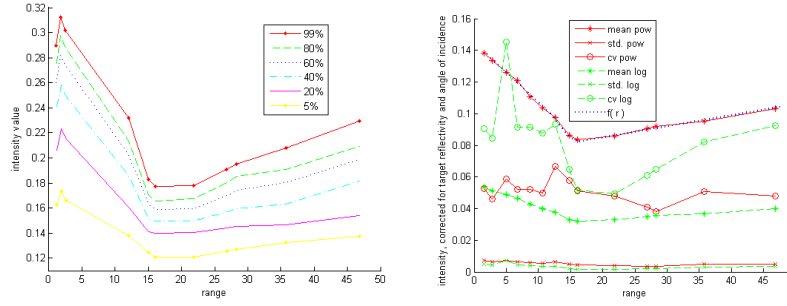

Figure 4. left: data of **Ex3** showing intensity against range, separated by target reflectivity. Right: intensity of **Ex1-5**, corrected by functions of target reflectivity and angle of incidence. The solid line refers to an exponential model (pow),

the dashed line to a logarithmic model. For bins of 2m width the mean value of the corrected intensities, their standard deviation, and the coefficient of variation are shown. The function f(r) relates range to intensity.

One part of function F has thus been identified, and a second part relating the range to the corrected intensity is required. Polynomial models did not fit the curve in Fig. 4, right, well. The intensity values corrected for target reflectivity and angle of incidence show two linear parts, for distances shorter and longer than 16m, respectively. It shall be noted, that this does not mean, that the received optical power increases with longer ranges, as the (amplification) behavior of the detector is included, too. Two linear functions were fitted and a C1-smooth transition with weight functions was determined. The branch for shorter ranges is $I = -0.0038r + 0.145$, and the branch for longer ranges is $I = 0.0007r + 0.071$. The transition from one model to the next was set in the range interval from 12m to 18m. This function f(r) is plotted in Fig. 4, right, and $F(\rho, \alpha, r) = f(r) * (\rho \cos(\alpha))^{-0.16}$.

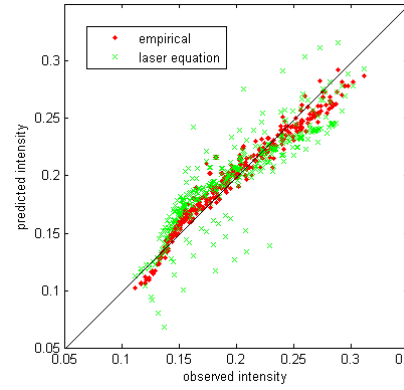

Figure 5: Predicted intensity vs. observed intensity. The (red) dots show the intensities predicted from the empirical model, the (green) crosses the intensities predicted from the laser range equation and the logarithmic amplification.

The σ_0 of the empirical model is 0.0108, which is only twice the spread in the intensity values.
The physically induced and the empirical model are compared graphically in Fig. 5. It shows a scatter plot of the observed intensity values against the predicted ones. An ideal model would show a 45° line. Both models do not only show a spread of values, which could be interpreted as random measurement errors, but also systematic deviations from this line.
Inverting the empirical relation and studying how well the reflectivity of the target can be computed from the observed intensity value draws a less optimistic picture. The r.m.s.e. with respect to reflectivity computed from range, incidence angle, and observed intensity value is ±23%. This is, again, about a factor two better, than for the physically induced model. However, there is clearly room for improvement.

4.4 Evaluation for Distance Offset and Background Radiation

It was investigated, if there is an influence of the target physical properties on the range measurement. Different authors have encountered such an effect during the execution of laser scanning projects. Experiments were also performed to quantify that effect based on color. With the targets available in this investigation, it is possible to isolate the effect of target reflectivity.
If different offsets are found based on target reflectivity, then the analysis does not allow to derive absolute offset values, as non can be assumed to be free of error. Therefore, only relative offsets can be determined. The plane of reference was the adjusting plane through all targets.
For the Lambertian targets the range of offsets was in the range of [-2mm,2mm]. A small trend could be observed with an offset of +0.5mm for lower intensity values, i.e. 0.1, reducing to a zero offset for higher intensity values, i.e. 0.3. It has to be noted that these specifications are well below the reported precision of the device. For the retroreflective targets, intensity about 0.7, and offsets of +2cm were observed, i.e. the points were lying 2cm closer to the scanner. No range dependence was observed in this effect.
The experiments **Ex4,5** were used to investigate, if there is an influence of ambient light on the intensity measurement. The experiments were performed in the lab with fluorescent light tubes and ordinary bulbs. Each measurement was performed with first the lights turned on and the the lights turned off. The intensity values with lights switched on are always higher than those with lights off.

The mean of all intensity values for **Ex4** was 0.2021, and for **Ex5** was 0.2015. The difference of 0.0006 is lower by a factor of ten than the spread of one intensity measurement. Reshetyuk (2006) observed for the Leica HDS 3000 in one experiment no systematic difference between scanning with and without ambient lighting.

5 CONCLUSIONS

For a terrestrial laser scanner, applying the pulse round trip time measurement principle, the so-called intensity values offered to the user, were investigated. The values for the investigated Riegl LMS-420i are generally in the range [0,1] and we could investigate the range [0.1,0.3] with Lambertian targets with reflectivity between 5% and 99%, observed at different ranges and at different angles of incidence.

In general, the intensity for the specific device we used have a standard deviation of 0.006, which is about 2% of their absolute value. A minimum of the spread was found at the intensity of 0.14, but we do not have an explanation for this effect. It was, however, observed at two different days and at different combinations of target reflectivity, range, and incidence angle.

The laser range equation was used to predict the intensity values. Experiments in which primarily the target reflectivity and the angle of incidence varied, but the range was kept close to 5m, it could be applied successfully. However, a logarithmic amplification of the detector had to be assumed. Under these circumstances, the observed intensity could be predicted with a r.m.s.e. of ±0.0140. If the span of range values included in the analysis increased, so did the r.m.s.e. For the experiments in the range of 2m to 50m it becomes ±0.0216. Including also shorter ranges (below system specification), down to 1.2m, increases the r.m.s.e. to ±0.0227. The systematic deviations found in this model can be interpreted in two ways. Firstly, the assumptions associated with the laser range equation do not hold. These assumptions include: operation in the far field, and an coincident field of view of emitter and detector. Another option is that the amplification of the signal does not follow a simple (linear or logarithmic) model, but is more complex.

An empirical model relating the known target reflectivity, computed angle of incidence, and observed range to the intensity, resulted in a r.m.s.e. of ±0.0108, predicting the intensities better. This model is entirely data driven and does not consider physical laws and amplification of the detector separately. The model is valid for the specific device used, and was derived for ranges in the interval [1.2m,48m], Lambertian target reflectivity [5%,99%], and angle of incidence [0°,70°].

For retroreflective targets an offset of 2cm was observed, with the points lying too close to the scanner. In our experiments we did not find offsets larger than 1mm for the Lambertian targets. One experiment was performed to investigate the influence of background light. While a small trend could be observed, it was below the noise level of a single intensity measurement by a factor of ten.

Generally, the experiments show, that the laser range equation must not be used blindly to predict the intensity reported by a laser scanning device. However, models can be derived with dedicated experiments. The experiment setup should be improved to cover the entire spectrum of ranges that can be measured with a laser scanner under test. The use of the surface reflecting targets with calibrated reflectivity is judged positively. It gave confidence in observing only reflectivity behavior at the wavelength of the scanner, and not a mixture of surface properties as angular scattering characteristics, propagation of the energy into the target, and reflectivity, but of reflectivity alone.

Future experiments should involve larger ranges, lower intensities by rotation of the targets at larger ranges, different scanners of the same model, but also from different vendors, and finally using different range measurement principles.

We conclude that improved models will allow exploiting the intensity values better, e.g. in the determination of target physical properties.

Acknowledgement: Measurements were performed with the Riegl laser scanner of the Vienna University of Technology ILSCAN group. Data acquisition was performed fast, reliable, and accurate by our students Nicole Hirtl and Stefan Niedermayr.

REFERENCES

1. Bae and Lichti, 2005. A framework for position uncertainty of unorganised three-dimensional point clouds from near-monostatic laser scanners using covariance analysis. IAPRS XXXVI 3/W19, Enschede, Netherlands.
2. Bucksch, van Ree, 2007. Personal communication. Delft Institute of Earth Observation and Space systems.
3. Godin et al, 2001. An Assessment of Laser Range Measurement on Marble Surfaces. Proc. 5th Conf. Optical 3D Measurement Techniques, Vienna, Austria.
4. Hanke, Grussenmeyer, Grimm-Pitzinger, Weinold, 2006. First experiences with the Trimble GX scanner. IAPRS XXXVI/5, Dresden, Germany.
5. Höfle, Rutzinger, Pfeifer, 2006. Technical Report, Innsbruck University, Department of Geography.
6. Jelalian, 1992. Laser Radar Systems. Artech House.
7. Jutzi, Stilla, 2003. Analysis of laser pulses for gaining surface features of urban objects. 2nd GRSS/ISPRS Joint Workshop on Remote Sensing and data fusion on urban areas, URBAN 2003.
8. Jutzi, Stilla, 2006. Range determination with waveform recording laser systems using a Wiener Filter. ISPRS Journal of Photogrammetry and Remote Sensing 60.
9. Reshetyuk, 2006. Investigation and calibration of pulsed time-of-flight terrestrial laser scanners. Ph.D. thesis, Royal Institute of Technology (KTH), Division of Geodesy, Stockholm, Sweden.
10. Riegl, 2007. http://www.riegl.com. Accessed May 2007.
11. Valanis, Tsakiri, 2004. Automatic target identification for laser scanners. IAPRS XXXV, Istanbul, Turkey.
12. Wagner, Ullrich, Ducic, Melzer, Studnicka, 2006. Gaussian Decomposition and Calibration of a Novel Small-Footprint Full-Waveform Digitising Airborne Laser Scanner. ISPRS Journal of Photogrammetry and Remote Sensing 60.
13. Weitkamp, 2006. Lidar: Range-Resolved Optical Remote Sensing of the Atmosphere. Springer.